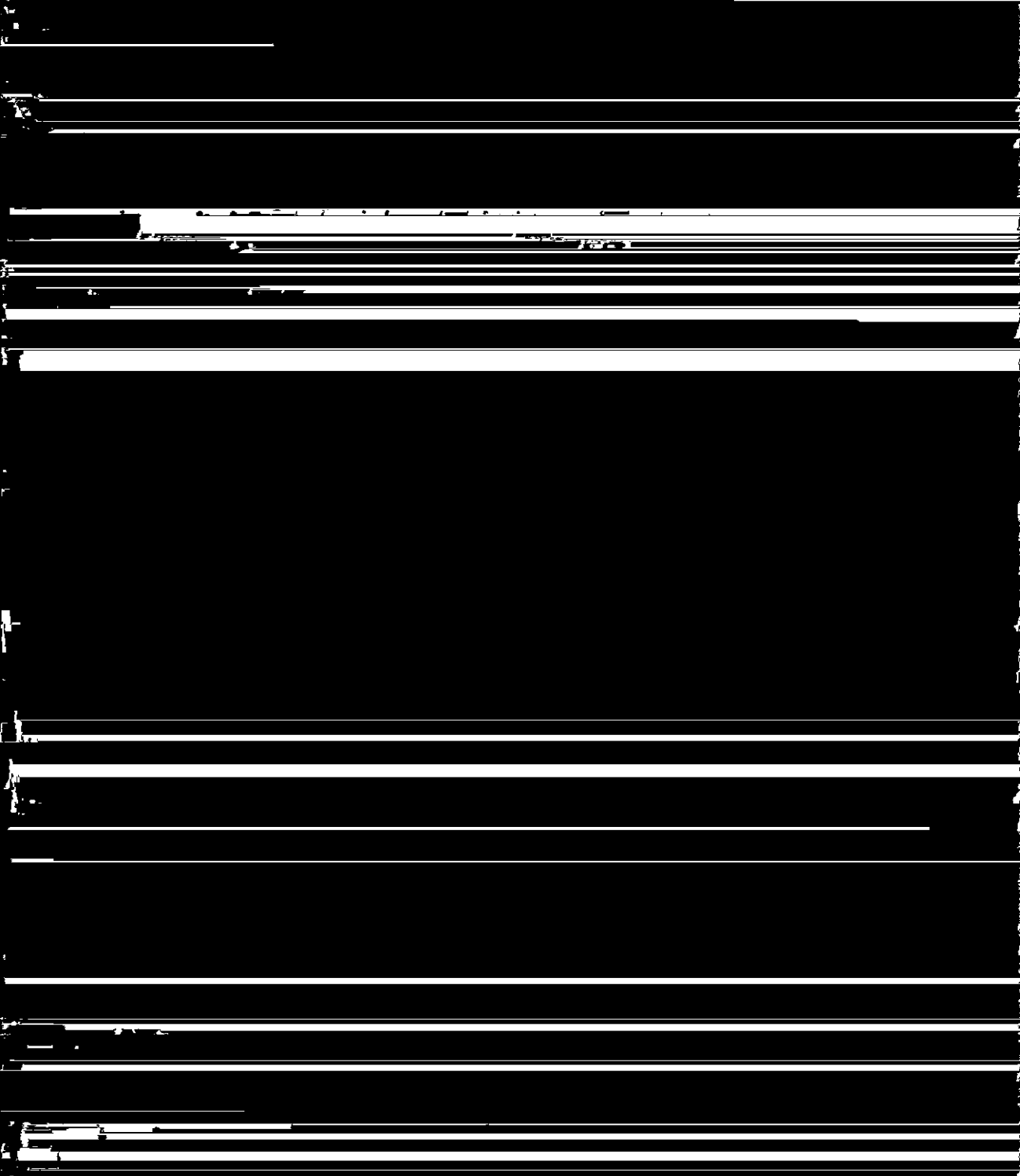


the Ag–Au system

Z W Lu†, Barry M Klein† and Alex Zunger‡

† Department of Physics, University of California, Davis, CA 95747, USA

atom, and (2) a set of interaction energies $\{J_{ij}\}$ among the various sites belonging to a



expansion techniques [1, 27-30]

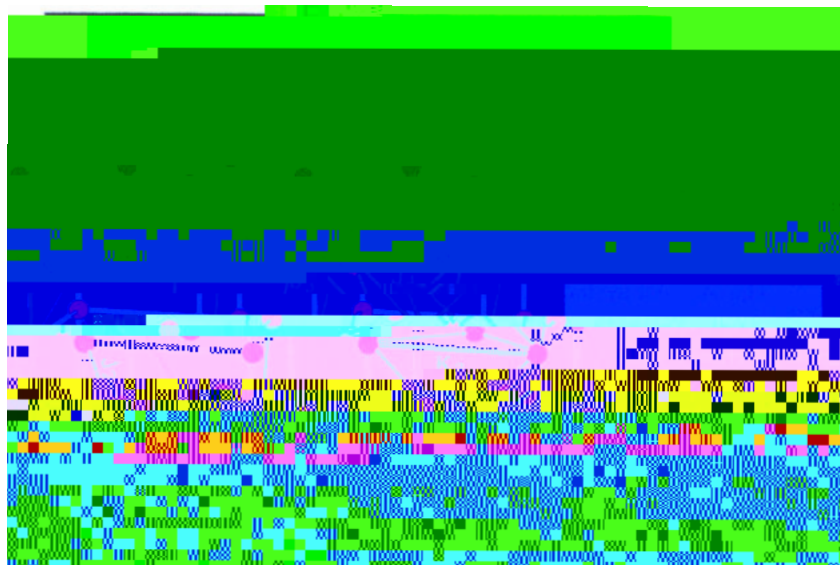
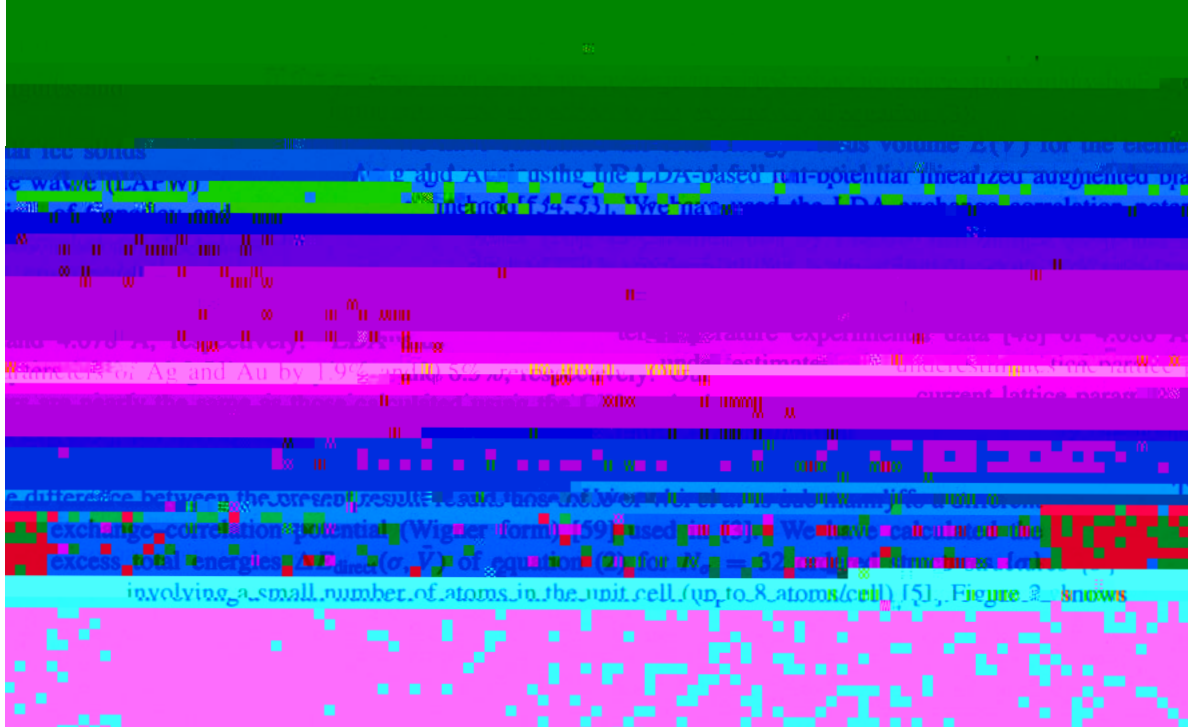


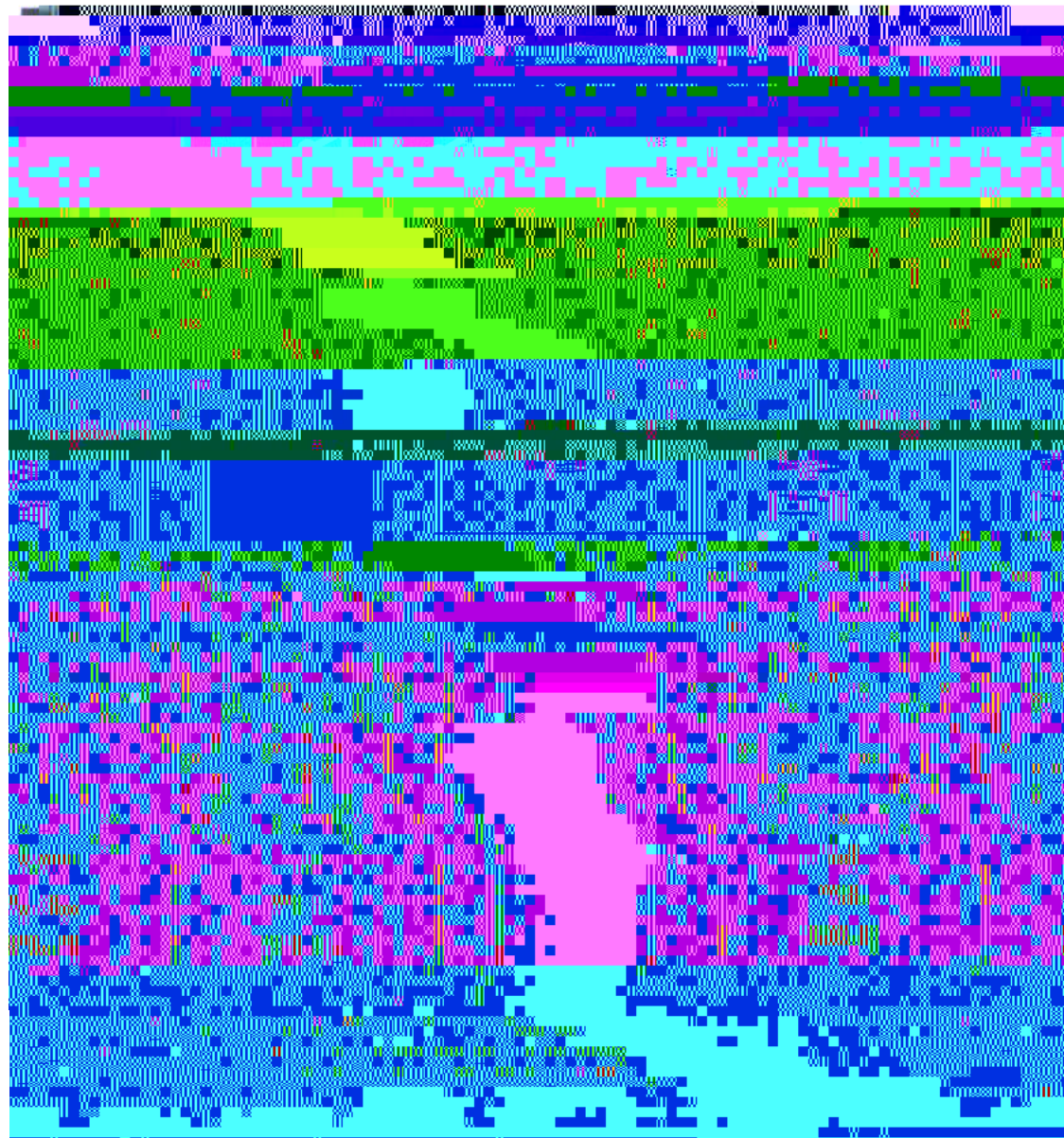
Figure 1. Geometric figures used in our cluster expansion. The expansion includes one-body figures, three-body figures, and four-body figures. See table 3 for the definition of the figure coordinates.

many-body terms). We determine the N_J interaction parameters $\{J_F\}$ by mapping N_σ directly calculated $\Delta E_{\text{direct}}(\sigma)$ values onto $\Delta E_{\text{CE}}(\sigma)$ of equation (3) through a least-squares fitting procedure, i.e. by minimizing

$$\sum_{\sigma}^{N_\sigma} (\Delta E_{\text{direct}}(\sigma) - \Delta E_{\text{CE}}(\sigma))^2 = \text{min} \quad (4)$$

Convergence is tested by applying equation (3) to a series of structures $\{\sigma_i\}$, not used in constructing the cluster expansion for equation (3). We find the following





examples of geometrically simple face-based ordered structures using our disorder circulator. Table 1 gives many examples of these structures. Most of these structures can be described by a period A_mB_n superlattices along some orientation as shown in figure 2 and calculated for ordered structures. The calculations for ordered structures are all carried out of the surface criticality.

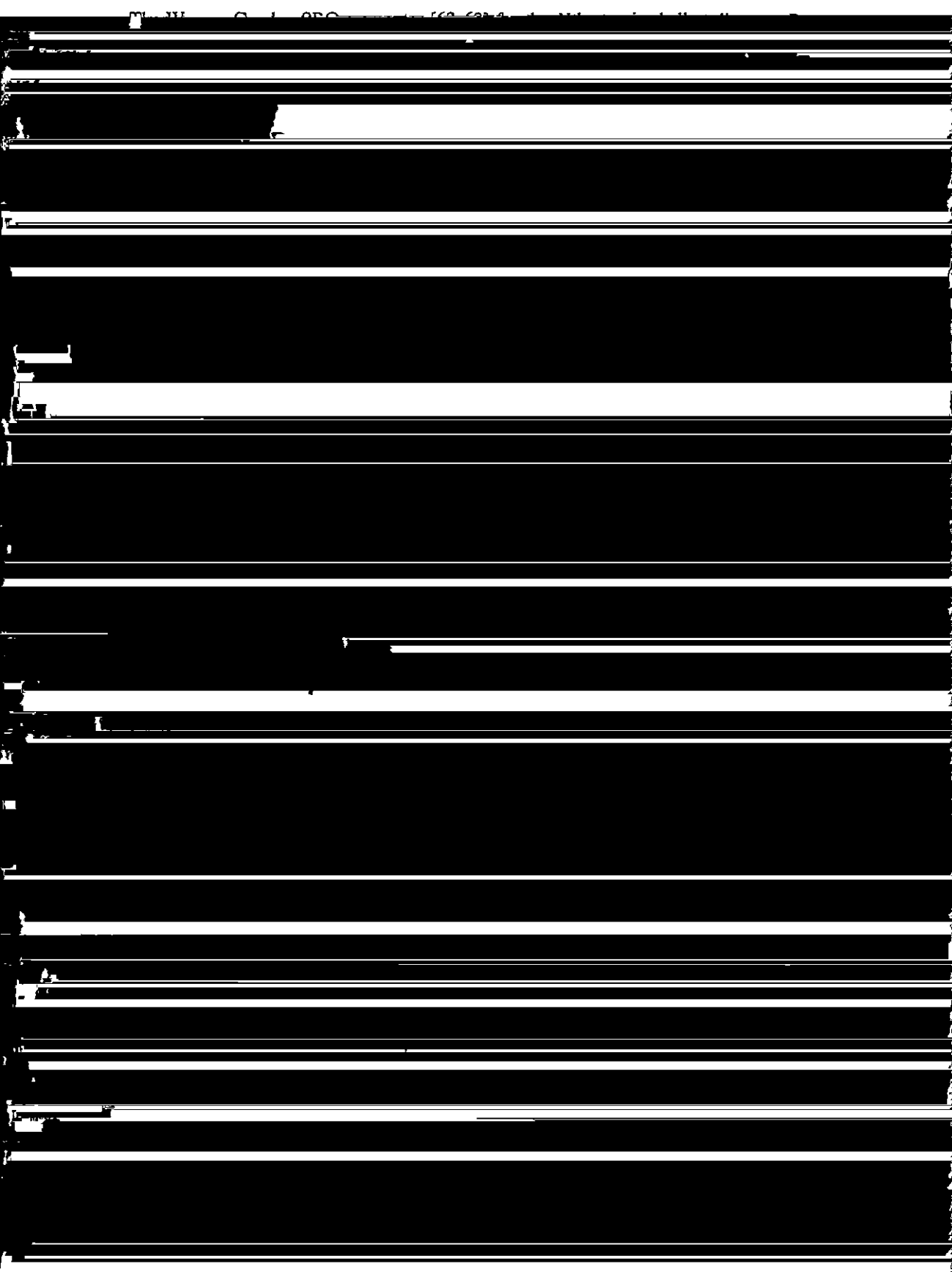
structure by ~ 15 meV/atom). To obtain

Au system relaxation lowers the energy of the L_{10} scheme that is geometrically equivalent. To obtain

Table 1. The directly calculated LAPW excess energies $\Delta E_{\text{direct}}(\sigma)$ (error $\sim \pm 2$ meV/atom) (equation (2)), the cluster-expanded energy $\Delta E_{\text{cr}}(\sigma)$ (equation (3)), and the prediction error

System	$\Delta E_{\text{direct}}(\sigma)$ (meV/atom)	$\Delta E_{\text{cr}}(\sigma)$ (meV/atom)	Prediction error (%)
Li ₂	-0.2	-0.2	0
Li ₃	-0.2	-0.2	0
Li ₄	-0.2	-0.2	0
Li ₅	-0.2	-0.2	0
Li ₆	-0.2	-0.2	0
Li ₇	-0.2	-0.2	0
Li ₈	-0.2	-0.2	0
Li ₉	-0.2	-0.2	0
Li ₁₀	-0.2	-0.2	0
Li ₁₁	-0.2	-0.2	0
Li ₁₂	-0.2	-0.2	0
Li ₁₃	-0.2	-0.2	0
Li ₁₄	-0.2	-0.2	0
Li ₁₅	-0.2	-0.2	0
Li ₁₆	-0.2	-0.2	0
Li ₁₇	-0.2	-0.2	0
Li ₁₈	-0.2	-0.2	0
Li ₁₉	-0.2	-0.2	0
Li ₂₀	-0.2	-0.2	0
Li ₂₁	-0.2	-0.2	0
Li ₂₂	-0.2	-0.2	0
Li ₂₃	-0.2	-0.2	0
Li ₂₄	-0.2	-0.2	0
Li ₂₅	-0.2	-0.2	0
Li ₂₆	-0.2	-0.2	0
Li ₂₇	-0.2	-0.2	0
Li ₂₈	-0.2	-0.2	0
Li ₂₉	-0.2	-0.2	0
Li ₃₀	-0.2	-0.2	0
Li ₃₁	-0.2	-0.2	0
Li ₃₂	-0.2	-0.2	0
Li ₃₃	-0.2	-0.2	0
Li ₃₄	-0.2	-0.2	0
Li ₃₅	-0.2	-0.2	0
Li ₃₆	-0.2	-0.2	0
Li ₃₇	-0.2	-0.2	0
Li ₃₈	-0.2	-0.2	0
Li ₃₉	-0.2	-0.2	0
Li ₄₀	-0.2	-0.2	0
Li ₄₁	-0.2	-0.2	0
Li ₄₂	-0.2	-0.2	0
Li ₄₃	-0.2	-0.2	0
Li ₄₄	-0.2	-0.2	0
Li ₄₅	-0.2	-0.2	0
Li ₄₆	-0.2	-0.2	0
Li ₄₇	-0.2	-0.2	0
Li ₄₈	-0.2	-0.2	0
Li ₄₉	-0.2	-0.2	0
Li ₅₀	-0.2	-0.2	0
Li ₅₁	-0.2	-0.2	0
Li ₅₂	-0.2	-0.2	0
Li ₅₃	-0.2	-0.2	0
Li ₅₄	-0.2	-0.2	0
Li ₅₅	-0.2	-0.2	0
Li ₅₆	-0.2	-0.2	0
Li ₅₇	-0.2	-0.2	0
Li ₅₈	-0.2	-0.2	0
Li ₅₉	-0.2	-0.2	0
Li ₆₀	-0.2	-0.2	0
Li ₆₁	-0.2	-0.2	0
Li ₆₂	-0.2	-0.2	0
Li ₆₃	-0.2	-0.2	0
Li ₆₄	-0.2	-0.2	0
Li ₆₅	-0.2	-0.2	0
Li ₆₆	-0.2	-0.2	0
Li ₆₇	-0.2	-0.2	0
Li ₆₈	-0.2	-0.2	0
Li ₆₉	-0.2	-0.2	0
Li ₇₀	-0.2	-0.2	0
Li ₇₁	-0.2	-0.2	0
Li ₇₂	-0.2	-0.2	0
Li ₇₃	-0.2	-0.2	0
Li ₇₄	-0.2	-0.2	0
Li ₇₅	-0.2	-0.2	0
Li ₇₆	-0.2	-0.2	0
Li ₇₇	-0.2	-0.2	0
Li ₇₈	-0.2	-0.2	0
Li ₇₉	-0.2	-0.2	0
Li ₈₀	-0.2	-0.2	0
Li ₈₁	-0.2	-0.2	0
Li ₈₂	-0.2	-0.2	0
Li ₈₃	-0.2	-0.2	0
Li ₈₄	-0.2	-0.2	0
Li ₈₅	-0.2	-0.2	0
Li ₈₆	-0.2	-0.2	0
Li ₈₇	-0.2	-0.2	0
Li ₈₈	-0.2	-0.2	0
Li ₈₉	-0.2	-0.2	0
Li ₉₀	-0.2	-0.2	0
Li ₉₁	-0.2	-0.2	0
Li ₉₂	-0.2	-0.2	0
Li ₉₃	-0.2	-0.2	0
Li ₉₄	-0.2	-0.2	0
Li ₉₅	-0.2	-0.2	0
Li ₉₆	-0.2	-0.2	0
Li ₉₇	-0.2	-0.2	0
Li ₉₈	-0.2	-0.2	0
Li ₉₉	-0.2	-0.2	0
Li ₁₀₀	-0.2	-0.2	0

Table 2. This table illustrates the effects of k -point sampling on the calculated ΔE_{direct} (in meV/atom) of some ordered compounds. The structures are defined in table 1. We have used the equivalent k -point sampling scheme of [60]; these two k -point sets are equivalent to 60 and 408 fcc special k -points, respectively (see [58]). We also give the actual number of k -points, N_k , in the irreducible zone for a particular structure.



(AB). Using this original Connolly-Williams procedure, we obtained an average prediction error of $\delta_{PE} = 1.6$ meV/atom and a maximum prediction error of 4.4 meV/atom for 27 other structures that are not used in obtaining the interaction J values. The prediction errors for some specific structures are unsatisfactory. For example δ_{PE} are 4.4, 2.4, 3.0, 2.6 meV/atom, for structures '40', $\gamma 2$, $D\bar{O}_{22}$ (AgAu_3), and W3, respectively (larger than the estimated error of direct LDA calculation of 2 meV/atom). The large error for '40' and $D\bar{O}_{22}$ is because the Connolly-Williams set of interactions creates a spurious degeneracy

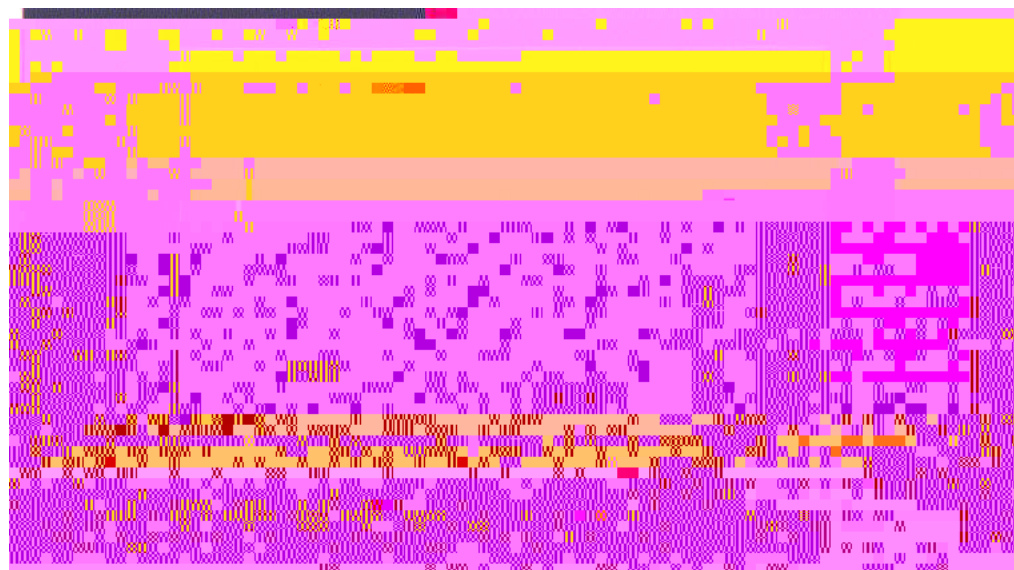


Figure 3. This figure illustrates the interaction energies (including the degeneracy $D(FJ)$) used in this work (figure 1) for fit I (table 3). The interaction energies for fit II are nearly indistinguishable on this scale. Note that the nearest-neighbor pair interaction J_1 is dominant.

²⁵ Note S contains a definition of the 'figures' F used in our cluster expansion in terms of the



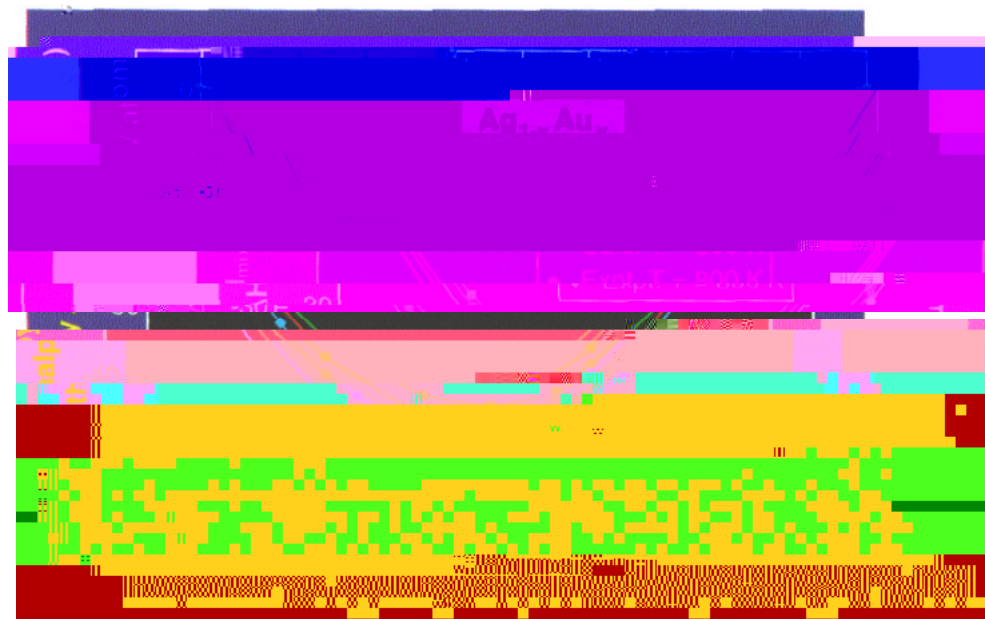


Figure 4. Calculated and measured mixing energy for $\text{Ag}_{1-x}\text{Au}_x$. The $T = 800 \text{ K}$, Jozenggs) are cited from [23]. We give the calculated values at

$T = 800 \text{ K}$ and the measured values at $T = 800 \text{ K}$.

Table 4. The experimental [23] and calculated (fit by Ag_{1-x}Au_x mixing enthalpy ΔH_{mix} (me/atom) using (i) Monte Carlo simulation to $T \leq 800 \text{ K}$ (including the short-range effects and (ii) equation (6) corresponding to the completely random alloy, all $\langle f_i f_j \rangle \sim 1/4$)

order $\sim x$	$\Delta H(x, T = 800 \text{ K})$		$\Delta H(x, T \rightarrow \infty)$	
	Experiment $T_c = 800 \text{ K}$	Monte Carlo $T \leq 800 \text{ K}$	Calc. (equation (6)) $T \rightarrow \infty$	Calc. (equation (6)) $T = 800 \text{ K}$
0.0	0.0	0.0	0.3	0.3
0.3	-0.1	-0.1	-0.1	-0.1



Figure 5. Calculated mixing enthalpy $\Delta H(x, T)$ for $\text{Ag}_{1-x}\text{Au}_x$ as a function of composition x for different temperatures.



Figure 6. Calculated mixing enthalpy $\Delta H(x, T)$ for $\text{Ag}_{1-x}\text{Au}_x$ as a function of composition x for different temperatures.

Table 5. The order-disorder phase transition temperatures T_c for $\text{Ag}_{1-x}\text{Au}_x$ alloys at $x = \frac{1}{4}$, $\frac{1}{2}$, and $\frac{3}{4}$. The calculated results were obtained using N_J interactions, solving the ensuing Ising model with the Monte Carlo (MC) method or with the cluster variation method (CVM). The 'measured' data were obtained by (i) using an inverse Monte Carlo method to extract three composition-dependent effective pair interactions from the short-range order data of the Georgopoulos-Cohen (GC) and Börner-Sparks (BS) analyses and (ii) subjecting these effective interactions to a direct Monte Carlo simulation.

		Ag ₃ Au <i>L</i> 1 ₂	AgAu <i>L</i> 1 ₀	AgAu ₃ <i>L</i> 1 ₂
Calculated (K)				
Present, fit I	$N_J = 12$; MC	155	210	225
Wei <i>et al</i> ^a	$N_J = 5$; CVM	120	240	200
Mohri <i>et al</i> ^b	$N_J = 5$; CVM	152	177	183
'Measured' (K)				
Schönfeld <i>et al</i> (BS) ^c	$N_J = 3$; MC	115	115	155
Schönfeld <i>et al</i> (GC) ^d	$N_J = 3$; MC	165	165	210
Norman and Warren ^e		90		
Ziesemer ^f			168	

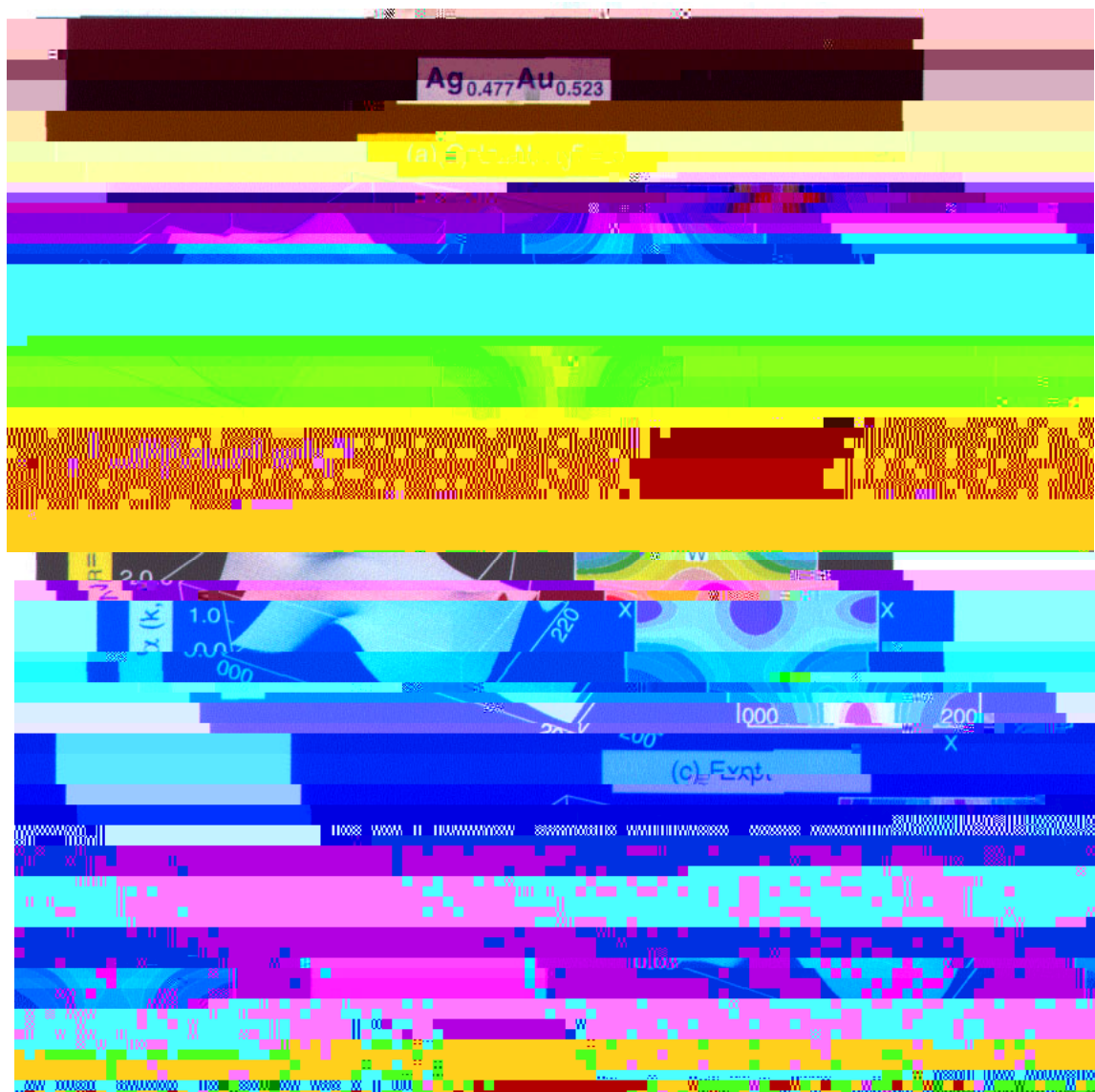


Figure 5. (a) Calculated SRO diffuse-scattering intensity for $\text{Ag}_{0.477}\text{Au}_{0.523}$ using Connolly Williams set of nearest-neighbor $N_f = 5$ interaction energies, (b) calculated SRO map using our set of $N_f = 12$ interaction energies, and (c) experimental 10^3 times diffuse-scattering intensity due to silver segregation in $\text{Ag}_{0.477}\text{Au}_{0.523}$, which were Fourier synthesized.



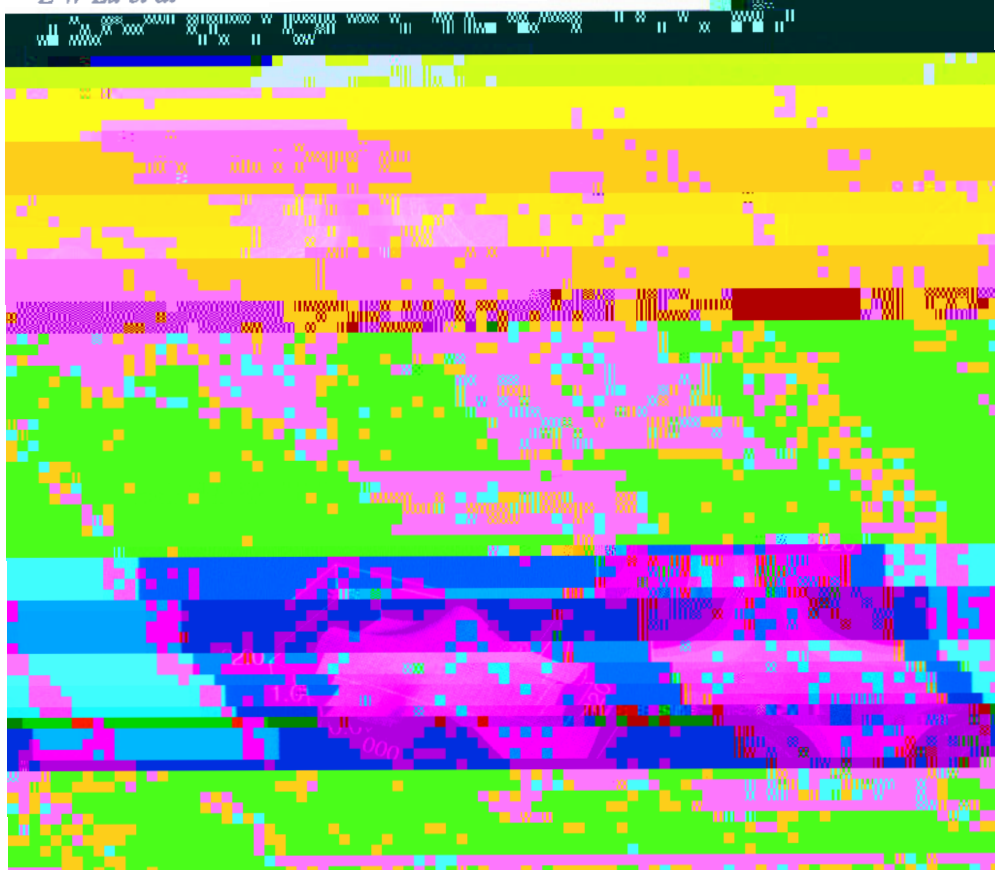


Figure 6. Calculated (a) and experimental (b) [15] diffuse-scattering intensities due to short-range order in the Ni₃Al₂ phase. The calculations were performed by Fourier synthesis in reciprocal space $\alpha(\mathbf{K}_{lmn})$ (including $\alpha(\mathbf{K}_{000}) = 1$ for both experiment and theory). The calculation was done at $T = 600$ K, while the experiment was performed on a sample that was homogenized at $T = 1173$ K and later aged at $T = 513$ K.



3.4. $T = 0$ ground state structures

The ground-state problem can be solved using the linear programming method [17], or for alloys that may not have complete regularities, for the ground state were solved in CKA

difference at $x = 0.5$ is -4.4 meV/atom, correlating with a fairly pronounced peak at the X point for $\alpha_{\text{SRO}}(k)$ at $x = 0.523$.

4. Conclusions

We have demonstrated here that accurate alloy properties can be obtained from *ab initio* calculated total energies for 20 atoms over a wide range of compositions.

- [26] Bozzolo G, Ferrante J and Smith J R 1992 *Phys. Rev. B* **45** 493
- [27] Terakura K, Oguchi T, Mohri T and Watanabe K 1987 *Phys. Rev. B* **35** 2169-73
- [28] Mohri T, Terakura K, Oguchi T and Wantanabe K 1988 *Acta Metall. Mater.* **36** 547-53
- [29] Mohri T, Terakura K, Takizawa S and Sanchez J M 1991 *Acta Metall. Mater.* **39** 493-501
- [30] Mohri T, Takizawa S and Terakura K 1992 *J. Phys.: Condens. Matter.* **5** 1479-90